Available online at www.sciencedirect.com
ScienceDirect
Scripta Materialia 57 (2007) 285–288
Scripta MATERIALIA
www.elsevier.com/locate/scriptamat

The strengthening effect of icosahedral phase on as-extruded Mg–Li alloys

D.K. Xu,[a,b] L. Liu,[a] Y.B. Xu[a] and E.H. Han[b,*]

[a] *Shenyang National Laboratory for Materials Science, Institute of Metal Research, Chinese Academy of Sciences, Shenyang 110016, China*
[b] *Environmental Corrosion Center, Institute of Metal Research, Chinese Academy of Sciences, Shenyang 110016, China*

Received 31 October 2006; revised 30 December 2006; accepted 7 March 2007
Available online 11 May 2007

Through investigating the mechanical properties of three kinds of Mg–Li–Zn–Y alloys, a strengthening method, i.e. introducing I-phase (Mg_3Zn_6Y, icosahedral quasicrystal structure) in the matrix of Mg–Li alloys, for as-extruded Mg–Li alloys has been demonstrated. The tensile results indicate that I-phase can effectively strengthen the alloys. The substantial enhancement of strength has been explained by microstructure changes.

Keywords: I-phase; Mg–Li alloy; Mechanical properties

Alloying magnesium with lithium of extremely low density ($0.534\ \mathrm{g\,cm^{-3}}$) can further reduce the weight of Mg alloys. However, based on the previous results listed in Table 1, the strength of Mg–Li alloys is very low [1,2]. Generally, previous strengthening methods, such as adding Zn or Al alloying elements and severe plastic deformation (hot extrusion or equal channel angular extrusion), cannot make the ultimate tensile strength (UTS) of Mg–Li alloys exceed 200 MPa.

On the other hand, it has been reported that Mg–Zn–Y alloys containing I-phase (Mg_3Zn_6Y, icosahedral quasicrystal structure) as a secondary phase exhibit good mechanical properties at both room temperature and elevated temperature [3]. Depending on the volume fraction of I-phase, Mg–Zn–Y–Zr alloys can have yield strength from 150 to 450 MPa at room temperature [4]. Previous studies [5–9] indicated that the existence of I-phase in Mg–Zn–Y or Mg–Zn–Y–Zr alloys was closely dependent on the Zn/Y weight ratio. Literature [7] suggested that when the Zn/Y ratio exceeded 4.38, element Y would exist almost completely as I-phase. When the Zn/Y ratio was above a certain value (>4.38), with increasing Y content, more I-phase would be formed in the Mg matrix.

Based on the analysis of these two alloy systems mentioned above, two questions can be asked: (i) can I-phase be introduced into Mg–Li alloys? (ii) If I-phase can be introduced, will the mechanical properties of Mg–Li alloys be greatly improved? Therefore, in this work, three alloys (with Zn/Y ratios higher than 5), namely Mg–8% Li–3% Zn–0.6% Y, Mg–8% Li–6% Zn–1.2% Y and Mg–8% Li–9% Zn–1.8% Y, were prepared. By investigating the mechanical properties of the alloys, the two questions will be answered.

The materials used in this study were as-extruded Mg–Li–Zn–Y magnesium alloys with different Zn and Y contents, which were prepared using specific technology in the Magnesium Alloy Research Department of IMR, China. Using inductively coupled plasma atomic emission spectrum apparatus, the chemical compositions of alloys I–III were determined, and these are listed in Table 2. The extrusion ratio was 10:1.

Phase analysis was determined with a D/Max 2400 X-ray diffractometer (XRD). Microstructures of the as-cast alloys I–III were examined by scanning electron microscopy (SEM; XL30-FEG-ESEM). Tensile bars with a gauge length of 25 mm and 5 mm in diameter were machined from the alloys. The axial direction of the tensile specimens was parallel to the extruded direction. Tensile experiments were conducted on an MTS (858.01 M) testing machine with a constant strain rate of $1\times10^{-3}\ \mathrm{s^{-1}}$ at room temperature. SEM (XL30-FEG-ESEM)

---

* Corresponding author. E-mail: ehhan@imr.ac.cn

1359-6462/$ - see front matter © 2007 Acta Materialia Inc. Published by Elsevier Ltd. All rights reserved.
doi:10.1016/j.scriptamat.2007.03.017

Table 1. Summary of the mechanical properties of the different Mg–Li alloys (tested at room temperature)

Condition	As-extruded state			Equal channel angular extrusion		
	$\sigma_{0.2}$ (MPa)	UTS (MPa)	Elongation (%)	$\sigma_{0.2}$ (MPa)	UTS (MPa)	Elongation (%)
Mg–11% Li–1% Zn [1]	96	133	60	150	175	35
Mg–9% Li–1% Zn [1]	100	141	56	160	182	31
Mg–9% Li–1% Zn–0.2% Mn [1]	90	130	70	140	165	22
Mg–9% Li–1% Zn–1% Al–0.2% Mn [1]	105	150	60	145	180	24
Mg–9% Li–1% Zn–3% Al–0.2% Mn [1]	110	161	50	130	180	27
Mg–3.3% Li [2]	69	160	18	113	200	33

Table 2. Chemical composition and the mechanical properties of the as-extruded Mg–Li–Zn–Y alloys

Normal alloys	Chemical composition (wt.%)				Zn/Y ratio	Mechanical properties		
	Mg	Zn	Y	Li		$\sigma_{0.2}$ (MPa)	UTS (MPa)	Elongation (%)
Alloy I	Bal	3.12	0.61	8.04	5.11	148	222	30.7
Alloy II	Bal	6.47	1.26	7.86	5.13	159	239	20.4
Alloy III	Bal	9.25	1.79	7.67	5.17	166	247	17.1

observations using either secondary electron imaging or backscattered electron imaging were made to determine the fracture characteristics and cracked I-phase on the fracture surfaces.

XRD analysis is shown in Figure 1. It reveals that for alloys I–III, the main phases are α-Mg, β-Li, LiMgZn and I-phase. Meanwhile, with the increase in Zn and Y content, the diffraction peak of W-phase will be gradually intensified. In addition, it has been reported [3,6,10] that I-phase could form interdendritic eutectic pockets with α-Mg. Therefore, an easy way to determine I-phase is by its morphology.

The microstructure observations of as-cast alloys I–III are shown in Figure 2. The figure shows that I-phase/α-Mg eutectic pockets preferentially form at the α-Mg/β-Li phase interfaces. With increasing Zn and Y contents, I-phase/α-Mg eutectic pockets can not only coarsen at the α-Mg/β-Li phase interfaces but also gradually form in the α-Mg matrix. Since element Y exists almost entirely in the form of I-phase, the quantity of I-phase for alloys is depended on Y content. Therefore, based on the variation of Y content, it can be deduced that the quantity of I-phase for alloy III is 3 and two times as much as that of alloys I and II, respectively. In addition, with increasing Zn content, especially for alloy III, many lamellar LiMgZn phases can be observed in the α-Mg matrix, as shown in Figure 2(d).

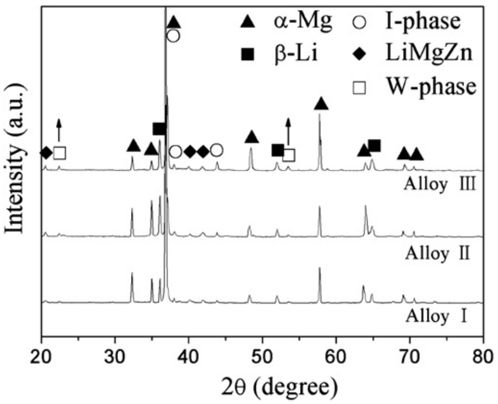

Figure 1. X-ray diffraction patterns of as-extruded Mg–Li–Zn–Y alloys. The arrows in the figure indicate the intensifying tendency of W-phase diffraction peak.

The stress–strain curves are shown in Figure 3. To describe and compare these conveniently, the mechanical properties of 0.2% proof yield stress ($\sigma_{0.2}$), UTS and elongation to failure for the alloys are listed in Table 2. It can be seen that the quantity of I-phase can effectively improve the yield strength and UTS of alloys. Comparing alloys I and III, with the quantity of I-phase increasing approximately 3-fold, the yield strength and UTS increase from 148 and 222 MPa to 166 and 247 MPa, respectively. Meanwhile, the plasticity of alloy III decreases greatly.

Previous research of Mg–Zn–Y–Zr alloys indicated [5,7,9] that with the quantity of W-phase increasing, the strength of alloys decreased. X-ray analysis indicates that for alloy II, W-phase can hardly be detected. Therefore, it can effectively avoid the influence of W-phase. To indicate the effect of I-phase on the mechanical properties of alloys, only the fracture of alloy II has been chosen to be observed. Figure 4 shows the secondary and backscattered SEM images of the fracture surfaces. The figure reveals that micro-cracks can form in the interior of big bulk I-phases.

Based on the Mg–Li–Zn ternary phase diagram [11], when Li content is between 6.0 and 9.5 wt.%, α-Mg and β-Li coexist and the Zn content in the solid solutions cannot exceed 2 wt.%. With decreasing solidification temperature, the solid solubility of Zn decreases gradually. Meanwhile, the Mg–Li–Y ternary phase diagram reveals [12] that the Y content in the solid solutions is very tiny. In addition, due to the interaction of elements Zn and Y, the solid solubility of Zn and Y is greatly decreased [13]. In this study, Li content of alloys I–III is about 8 wt.%. Therefore, as the solidification process continues, redundant Zn and Y (with a Zn/Y ratio higher than 4.38) will exist between α-Mg and β-Li phases and preferentially form I-phase at the α-Mg/β-Li phase interface. Certainly, I-phase can also form in the interior of α-Mg and β-Li matrix, as shown in Figure 2a–c. It has been reported that the melting temperature of I-phase eutectic pockets is about 450 °C [3,8,14,15].

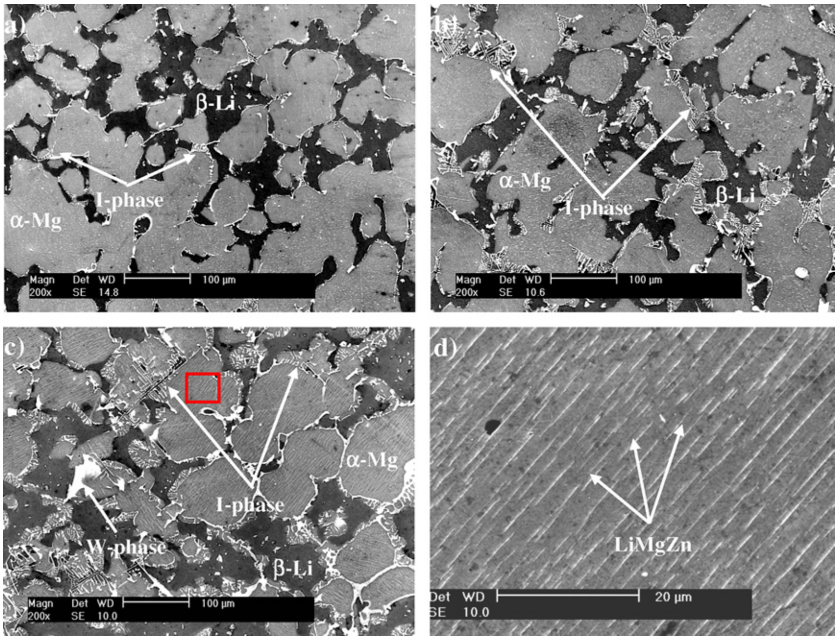

Figure 2. The microstructure of the as-cast Mg–Li–Zn–Y alloys: (a) alloy I, (b) alloy II, (c) alloy III and (d) high-magnification observation of the location squared in image (c).

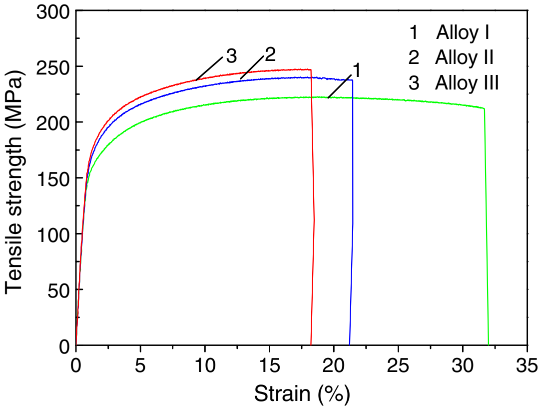

Figure 3. The stress–strain curves of the as-extruded Mg–Li–Zn–Y alloys.

Therefore, when the temperature is lower than 450 °C, the forming of I-phase will retard the further diffusion of Zn and Y. Especially for alloys II and III, more I-phase can form during solidification process, which will easily lead to the formation of areas with higher and lower Zn/Y ratios in the liquid phase. Therefore, the area (with lower Zn/Y ratio) cannot fully meet the requirement of forming I-phase and W-phase will be formed, whereas the area (with higher Zn/Y ratio) can successfully form I-phase and the redundant Zn will form a supersaturated solid solution in the α-Mg matrix. When the alloys are cooled down to room temperature, lamellar LiMgZn phases precipitate from the supersaturation solid solution, as shown in Figure 2(d). Previous research reported [16] that after T6 temper treatment (solid solution for 2.5 h at 500 °C plus 15 h of artificial ageing at 180 °C), Mg–Zn–Y phases (I-phase and W-phase) disappeared and rod-like $MgZn'$ precipitated from the supersaturated solid solution. In addition, the Mg–Li–Zn ternary phase diagram [11] indicates that when the contents of Mg and Zn are higher than about 40 at.%, Li will preferentially form LiMgZn phase with Zn and Mg. Therefore, the formation of LiMgZn can be divided into two steps: (i) the formation of an area of higher Zn content caused by rod-like $MgZn'$; and (ii) the diffusion of Li and the formation of LiMgZn. Based on the discussion above, I-phase can

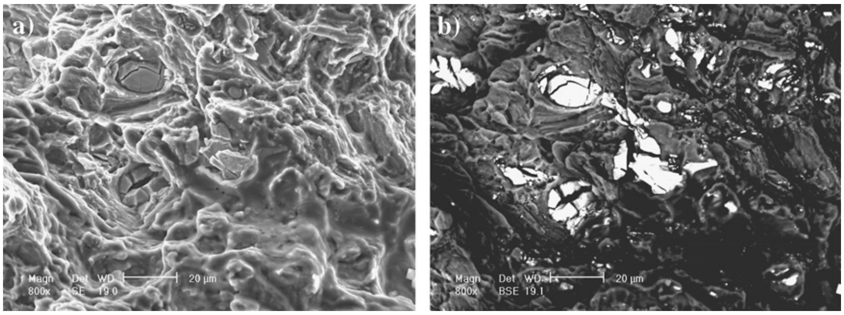

Figure 4. The SEM observation of cracked I-phase on the fracture surface for alloy II: (a) secondary and (b) backscattered SEM observation.

be successfully introduced into the matrix of Mg–Li alloys, which clearly answers the first question. Whether I-phase can effectively strengthen Mg–Li alloys or not will be discussed below.

It has been reported [3] that the interface layer of α-Mg, 3–5 nm thick, still preserved the orientation relationship with I-phase, and the coherency between I-phase and α-Mg could be achieved by introducing steps and ledges periodically along the interface. Therefore, the atomic bonding between I-phase and the hexagonal structure was rigid enough to be retained during severe plastic deformation. A study of as-cast Mg–Zn–Y–Zr alloys [5] suggested that the α-Mg/I-phase eutectic pockets could retard the basal slip and that no cracks could be observed at the α-Mg/I-phase interfaces. Compared with the tensile properties listed in Tables 1 and 2, this clearly suggests that introducing I-phase into the Mg matrix can effectively improve the strength of Mg–Li alloy. However, the stress–strain curves reveal that with the quantity of I-phase increasing, the difference in UTS between the alloys decreases greatly, as shown in Figure 3. The figure reveals that the difference of UTS between alloys I and II is about twice as great as that between alloys II and III, which can be ascribed to two main reasons. First, based on X-ray phase analysis (in Fig. 1) and the discussion of the phase-forming mechanism, the quantity of W-phase increases with increasing Zn and Y content, which degrades the strength of alloys, especially for alloy III. Secondly, due to the higher content of Zn and Y for alloys II and III, I-phase formed at the α-Mg/β-Li interfaces will be coarsened, leading to a large bulk I-phase after hot-extrusion processing. During the tensile testing, the higher stress concentration will occur around the large bulk I-phase, which degrades the strength of alloys. Figure 4 shows that at a certain stress level, micro-cracks will be formed in the interior of the large bulk I-phase to relieve the deformation incompatibility between I-phase and α-Mg matrix. This provides further evidence that α-Mg/I-phase interfaces are very strong. Furthermore, it also indicates that the size of the cracked I-phase is larger than 10 μm. Therefore, to fully exploit the potential strength of Mg–Li alloys, the quantity of existing W-phase and the size of I-phase must be strictly controlled.

By investigating three kinds of Mg–Li alloys, a strengthening method, i.e. introducing I-phase in the alloy matrix, has been demonstrated. The maximum UTS of the new exploited alloys can reach 250 MPa. Based on experimental results, two main factors influencing the strength of alloys can be determined: the quantity of existing W-phase and the size of I-phase. Therefore, it can be predicted that by controlling these two factors, the potential strength of Mg–Li alloys can be further improved.

This work was supported by National Science Fund of China (NSFC) project under Grant No. 50431020.

[1] Tien-Chan Chang, Jian-Yih Wang, Chun-Len Chu, Shyong Lee, Mater. Lett. 60 (2006) 3272–3276.
[2] T. Liu, Y.D. Wang, S.D. Wu, R. Lin Peng, C.X. Huang, C.B. Jiang, S.X. Li, Scripta Mater. 51 (2004) 1057–1061.
[3] D.H. Bae, S.H. Kim, D.H. Kim, W.T. Kim, Acta Mater. 50 (2002) 2343–2356.
[4] E.S. Park, S. Yi, J.B. Ok, D.H. Bae, W.T. Kim, D.H. Kim, in: Proceedings MRS Fall Meeting, Boston, MA, 2001.
[5] D.K. Xu, W.N. Tang, L. Liu, Y.B. Xu, E.H. Han, J. Alloy. Compd. 432 (2007) 129.
[6] Ju Yeon Lee, Do Hyung Kim, Hyun Kyu Lim, Do Hyang Kim, Mater. Lett. 59 (2005) 3801.
[7] D.K. Xu, L. Liu, Y.B. Xu, E.H. Han, J. Alloy. Compd. 426 (2006) 155.
[8] Ya Zhang, Xiaoqin Zeng, Liufa Liu, Chen Lu, Hantao Zhou, Qiang Li, Yanping Zhu, Mater. Sci. Eng. A 373 (2004) 320.
[9] D.K. Xu, L. Liu, Y.B. Xu, E.H. Han, Mater. Sci. Eng. A 443 (2007) 248.
[10] D.H. Bae, Y. Kim, I.J. Kim, Mater. Lett. 60 (2006) 2190.
[11] P.I. Kripyakevich, E.V. Mel'nik, in: P. Villars, A. Prince, H. Okamoto (Eds.), Ternary Alloy Phase Diagrams, ASM International, Materials Park, OH, 1997, p. 12227.
[12] M.E. Drits, L.S. Guzei, M.L. Kharakterova, A.A. Burgyin, in: P. Villars, A. Prince, H. Okamoto (Eds.), Ternary Alloy Phase Diagrams, ASM International, Materials Park, OH, 1997, p. 12224.
[13] E.M. Padezhnova, E.V. Mel'nik, R.A. Miliyevskiy, T.V. Dobatkina, V.V. Kinzhibalo, in: P. Villars, A. Prince, H. Okamoto (Eds.), Ternary Alloy Phase Diagrams, ASM International, Materials Park, OH, 1997, p. 12369.
[14] Xiaoqin Zeng, Ya Zhang, Chen Lu, Wenjiang Ding, Yingxin Wang, Yanpin Zhu, J. Alloy. Compd. 395 (2005) 213.
[15] D.H. Bae, M.H. Lee, K.T. Kim, W.T. Kim, D.H. Kim, J. Alloy. Compd. 342 (2002) 445.
[16] D.K. Xu, L. Liu, Y.B. Xu, E.H. Han, Mater. Sci. Eng. A 420 (2006) 322.